31st Congress of the International Council of the Aeronautical Sciences

Belo Horizonte, Brazil; September 09-14, 2018

A HYBRID LENGTH SCALE SIMILARITY SOLUTION FOR SWIRLING TURBULENT JETS

Geoffrey Andrews*
*Purdue University

Keywords: *Turbulent Jet, Similarity Solution, RANS, Aerodynamics*

Abstract

Approximate scaling laws for downstream properties of a swirling turbulent jet are estimated using the boundary layer approximations to the Navier-Stokes equations. The swirling jet is found to behave similarly to an equivalent non-swirling jet for low to moderate azimuthal velocities; in this regime the chief difference between swirling and non-swirling jets is an increased spreading rate and an increase in entrainment of ambient fluid for the former when compared to the latter. As azimuthal momentum flux increases, the flow becomes unstable and vortex breakdown occurs beyond a "critical" condition. Up until the critical point, the mean velocity profiles of this flow as a function of downstream distance can be predicted as a function of swirl using a hybrid length scale model; the predictions of this model match the available experimental data with reasonable accuracy.

1 Introduction

1.1 Overview

This report will present the scaling analysis of turbulent jets with swirl. Section 2 simplifies the Reynolds-averaged Navier-Stokes equations in cylindrical coordinate system and simplifies them using boundary layer approximations. Section 3 is dedicated to deriving the scaling analysis based on the assumption of an undetermined similarity solution. Unlike the analyses of previous work, the influence of swirl is considered and used to obtain the scaling relationships for mean velocity profiles. Section 4 presents comparisons between the scaling analysis and experimental data to verify that the analysis is reasonable.

1.2 Background

The swirling jet is a flow of great practical interest, particularly in the field of combustors for gas turbine engines, where the presence of swirl enhances turbulent mixing of fuel and air. However, the problem is not generally well-understood as the presence of azimuthal velocity complicates the familiar problem of the non-swirling jet. The combination of free jet and rotating flows presents several unique phenomena. Experiments indicate that weak to moderate levels of swirl increase the spreading rate of the jet, represented by a shift in the flow's virtual origin and increased entrainment of ambient fluid into the jet. As azimuthal velocity increases further, the jet forms a peculiar counter-rotating core, where fluid several jet diameters downstream moves with a reversed azimuthal motion. Beyond a certain "critical" point, the azimuthal velocity becomes overpowering. The bulk swirling motion of the jet distorts the vortex lines of the flow, resulting in a self-induced axial motion which cause the vortex lines to wrap around the jet and break up, leading to a total collapse of the vortical structure of the jet.

1.3 Prior Work

Due to the inherent complexity of both generating and measuring a swirling jet, work on the

topic has been relatively scarce; certainly, the flow is less well-understood than its more familiar non-swirling cousin. Chigier and Chervinsky [1] presented what is arguably the most comprehensive work on the topic, investigating the effect of swirl on velocity distribution. They showed that for low swirl numbers, axial velocity distributions took the expected Gaussian shape; however, at higher swirl numbers a counter-rotating vortex core formed resulting in reversed azimuthal flow which displaced the maximum velocity from the jet axis; for very strong swirl, reversed flow was measured. These trends can be seen clearly in Figure 1 below, taken from their 1967 paper.

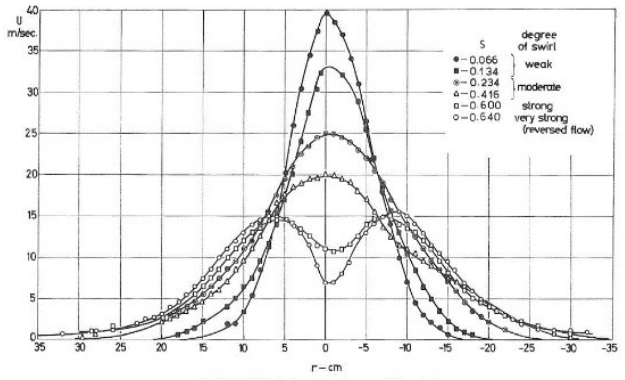

Fig. 1 : Axial velocity profiles downstream of a swirling jet for different values of swirl number S, from Chigier & Chervinsky [1]

A series of experimental studies by Facciolo [2] showed that swirl introduced into the jet flow increased both the entrainment of ambient fluid and the rate of spreading. This study also found that the decay of centerline velocity is significantly higher than for an irrotational jet and that it increases with higher swirl numbers. Facciolo also compared data from a Direct Numerical Simulation (DNS) to an earlier work by Rose [3] which measured a swirling jet using Laser Doppler Velocimetry (LDV). The two sets of data generally agreed, indicating that the introduction of swirl leads to a faster decay of axial velocity in jet flow.

In the experimental study of Shiri and George [4], it was shown that at low swirl numbers (approximately $S < 0.25$), there is no significant effect on the flow as compared to a non-swirling vortex; however, clear differences appear at higher swirl numbers. Other works suggest that beyond a certain critical value of swirl, vortex breakdown occurs and the flow can no longer be characterized as a coherent swirling jet. However, in the intermediate range of swirl which lies between the non-swirling case and vortex breakdown, the jet behaves similarly to an irrotational jet but with slightly different scaling of velocity, width, and turbulence parameters. This scaling has not been well-characterized beyond qualitative observations made in these experiments.

Several investigators have studied the problem of vortex breakdown in highly swirling jets; Ruith et al. [6] performed a numerical simulation which aptly demonstrated the phenomenon - the flow becomes increasingly helically disturbed at higher swirl Reynolds numbers, ultimately becoming fully chaotic. An experimental investigation by Billant et al [7] studied vortex breakdown in swirling jets, which explained the occurrence of reversed flow. They showed that a critical quantity of swirl exists, and that it is independent of Reynolds number and jet diameter. When the jet reaches this degree of swirl, breakdown starts - a stagnation point appears in the downstream turbulence region and gradually moves upstream to reach an equilibrium position. Their experiments also verified the critical swirl number to be in good agreement with the criterion derived in Escudier and Keller's theory [8] based on vortex breakdown in a tube. The critical swirl number can be predicted by:

$$\frac{1}{2}\frac{S_c J_1(S_c)}{J_2(S_c)} = \frac{1}{(r_t/r_c)^2 - 1}$$

Where S_c is the critical swirl number, J_1 and J_2 are Bessel functions of the first and second kind, respectively, and r_t and r_c are the radii of the tube and the core vortex, respectively. For the case of the swirling jet, r_t can be regarded as the radius of the jet exit.

D. Ewing [9] obtained similarity solutions for round turbulent jets with swirl. His paper showed that the axial velocity and the radial velocity are of the order of magnitude $1/x$, and the order of

magnitude of azimuthal velocity is $1/x^2$. Although his result demonstrated that the azimuthal velocity decays faster than the velocities on other two direction, his solution did not show the influence of swirl. This is the chief objective of the current study.

2 Governing Equations

The basis for this analysis is the Reynolds-Averaged Navier-Stokes Equations in cylindrical coordinates (x, r, θ). We define the axial velocity, azimuthal velocity and radial velocity as (U,V,W), respectively. We then proceed with a Reynolds velocity decomposition,

$$U = \overline{u} + u'$$

$$V = \overline{v} + v'$$

$$W = \overline{w} + w'$$

where the lowercase letters with bars denote the mean velocity and primed letters are fluctuating variables.
Assuming incompressible flow, the density ρ should be constant; we also assume that the flow is axisymmetric and steady. Thus, $\partial()/\partial t = 0$ and $\partial()/\partial\theta = 0$. In addition, for high Reynolds number turbulent flow, the molecular viscous term can be neglected in comparison with the turbulent viscous term. Based on the assumptions above, the Reynolds-averaged Navier-Stokes equations simplify as follows:

$$\frac{1}{r}\frac{\partial(r\overline{v})}{\partial r} + \frac{\partial\overline{u}}{\partial x} = 0 \tag{1}$$

$$\overline{v}\frac{\partial\overline{v}}{\partial r} + \overline{u}\frac{\partial\overline{v}}{\partial x} + \frac{\partial\overline{v'^2}}{\partial r} + \frac{\partial\overline{u'v'}}{\partial x} - \frac{1}{r}(\overline{w}^2 + \overline{w'^2} - \overline{v'^2}) = -\frac{1}{\rho}\frac{\partial\overline{p}}{\partial r} \tag{2}$$

$$\overline{u}\frac{\partial\overline{w}}{\partial x} + \overline{v}\frac{\partial\overline{w}}{\partial r} + \frac{\overline{w}\overline{v}}{r} + \frac{\partial\overline{u'w'}}{\partial x} + \frac{1}{r^2}\frac{\partial(r^2\overline{v'w'})}{\partial r} = 0 \tag{3}$$

$$\overline{u}\frac{\partial\overline{u}}{\partial x} + \overline{v}\frac{\partial\overline{u}}{\partial r} + \frac{1}{r}\frac{\partial(r\overline{u'v'})}{\partial r} + \frac{\partial\overline{u'^2}}{\partial x} = -\frac{1}{\rho}\frac{\partial\overline{p}}{\partial x} \tag{4}$$

Boundary layer approximations allow us to simplify the equations further. We start by nondimensionalizing the equations(*= dimensional quantity):

$$\begin{aligned} u &= u^*/U_0^* \\ v &= v^*/U_0^* \\ w &= w^*/U_0^* \\ r &= r^*/L_0^* \\ x &= x^*/L_0^* \\ p &= p^*/\rho^* U_0^* \\ \delta &= \delta^*/L_0^* << 1, \end{aligned}$$

Choosing u = O(1), $\frac{\partial}{\partial x}$ = O(1) Assume

$$\overline{u'^2} \sim \overline{v'^2} \sim \overline{w'^2} = O(q^2)$$

and $q = q^*/U_0^* << 1$. According to the continuity equation,

$$\frac{1}{r}\frac{\partial(r\overline{v})}{\partial r} = -\frac{\partial\overline{u}}{\partial x} = O(1)$$

$$\frac{L_0^*}{\delta^*}\frac{\delta^*}{\partial r^*}\frac{\partial}{\partial(r^*/\delta^*)}\left(\frac{r^*}{\delta^*}\frac{v^*}{U_0^*}\right) = O(1)$$

Thus,

$$\begin{aligned} \overline{u} &= O(1) \\ \frac{\partial}{\partial x} &= O(1) \\ \overline{v} &= O(\delta) \\ \frac{\partial}{\partial r} &= O\left(\frac{1}{\delta}\right) >> 1 \end{aligned}$$

For equation (4),

$$\begin{aligned} \overline{u}\frac{\partial\overline{u}}{\partial x} &\sim O(1) \\ \overline{v}\frac{\partial\overline{u}}{\partial r} &\sim O(1) \\ \frac{1}{r}\frac{\partial(r\overline{u'v'})}{\partial r} &\sim O(q^2/\delta) \\ \frac{\partial\overline{u'^2}}{\partial x} &\sim O(q^2) \end{aligned}$$

We can see that for the terms to all be of the same order of magnitude, $O(q^2) \sim O(\delta)$. The term $\frac{\partial \overline{u'^2}}{\partial x}$ can be neglected. Equation (4) thus becomes:

$$\overline{u}\frac{\partial \overline{u}}{\partial x} + \overline{v}\frac{\partial \overline{u}}{\partial r} + \frac{1}{r}\frac{\partial (r\overline{u'v'})}{\partial r} = -\frac{1}{\rho}\frac{\partial \overline{p}}{\partial x} \tag{5}$$

Meanwhile, for equation (2):

$$\begin{aligned}
\overline{v}\frac{\partial v}{\partial r} &\sim O(\delta)\\
\overline{u}\frac{\partial v}{\partial x} &\sim O(\delta)\\
\frac{\partial \overline{v'^2}}{\partial r} &\sim O(1)\\
\frac{\partial \overline{u'v'}}{\partial x} &\sim O(\delta)\\
\frac{\overline{w^2}}{r} &\sim O(1)\\
\frac{\overline{w'^2}}{r} &\sim O(1)\\
\frac{\overline{v'^2}}{r} &\sim O(1)\\
v &\sim O(\sqrt{\delta})
\end{aligned}$$

So $\overline{v}\frac{\partial v}{\partial r}, \overline{u}\frac{\partial v}{\partial x}, \frac{\partial \overline{u'v'}}{\partial x}$ are negligible. Equation (2) becomes:

$$\frac{\partial \overline{v'^2}}{\partial r} - \frac{1}{r}(\overline{w}^2 + \overline{w'^2} - \overline{v'^2}) = -\frac{1}{\rho}\frac{\partial \overline{p}}{\partial r}$$

For equation (3):

$$\begin{aligned}
\overline{u}\frac{\partial \overline{w}}{\partial x} &\sim O(\sqrt{\delta})\\
\overline{v}\frac{\partial \overline{w}}{\partial r} &\sim (\sqrt{\delta})\\
\frac{\overline{v}\cdot\overline{w}}{r} &\sim O(\sqrt{\delta})\\
\frac{\partial \overline{u'w'}}{\partial x} &\sim O(\delta)\\
\frac{1}{r^2}\frac{\partial (r^2\overline{v'w'})}{\partial r} &\sim O(1)
\end{aligned}$$

Then, equation (3) becomes:

$$\frac{1}{r^2}\frac{\partial (r^2\overline{v'w'})}{\partial r} = 0$$

Thus, the boundary-layer approximation provides us with the following equations:

Axial Momentum:

$$\overline{u}\frac{\partial \overline{u}}{\partial x} + \overline{v}\frac{\partial \overline{u}}{\partial r} + \frac{1}{r}\frac{\partial (r\overline{u'v'})}{\partial r} = -\frac{1}{\rho}\frac{\partial \overline{p}}{\partial x} \tag{6}$$

Radial Momentum:

$$\frac{\partial \overline{v'^2}}{\partial r} - \frac{1}{r}(\overline{w}^2 + \overline{w'^2} - \overline{v'^2}) = -\frac{1}{\rho}\frac{\partial \overline{p}}{\partial r} \tag{7}$$

Azimuthal Momentum:

$$\frac{1}{r^2}\frac{\partial (r^2\overline{v'w'})}{\partial r} = 0 \tag{8}$$

3 Scaling Analysis

A useful metric to analyze the degree of swirl present in a flow is the ratio of azimuthal to axial momentum flux. These two quantities can be calculated by integrating the axial and radial momentum boundary layer equations derived above:

$$\frac{d}{dx}\int_0^\infty r\left(\overline{u}^2 - \frac{\overline{w}^2}{2}\right)dr = \frac{d}{dx}G_\theta = 0 \tag{9}$$

$$\frac{d}{dx}\int_0^\infty r^2(\overline{u})(\overline{w})dr = \frac{d}{dx}G_\theta = 0 \tag{10}$$

The ratio of these momentum fluxes nondimensionalized by the jet exit radius R gives a dimensionless *swirl number*, S:

$$S = \frac{G_\theta}{G_x R}$$

The swirl number is convenient nondimensional parameter which can describe the degree of swirl present in different flows.

Axial Velocity

For a non-swirling jet, the centerline velocity can be expressed as a function of the axial distance downstream through the use of a similarity function:

$$U_c(r,x) = U_c(x)F(\eta)$$

where

$$\eta = \frac{r}{\delta}$$

However, the introduction of swirl adds a second relevant length scale characterized by the ratio of azimuthal to axial momentum flux:

$$L = \frac{G_\theta}{G_x}$$

If we assume that this swirling length scale is relevant to the scaling of the axial centerline velocity, then we can write a general expression for η as follows:

$$\eta = \frac{r}{[\delta^n L^m]^{\frac{1}{m+n}}}$$

This can be substituted into the axial conservation of momentum:

$$\frac{d}{dx}\left\{\int_0^\infty \int_0^{2\pi} \rho \overline{u}^2 r d\theta dr\right\} = 0$$

$$\int_0^\infty \int_0^{2\pi} \rho \overline{u}^2 r d\theta dr = C$$

$$\int_0^\infty \int_0^{2\pi} \rho U_c^2 F^2 \eta [\delta^n L^m]^{\frac{1}{m+n}} d\theta [\delta^n L^m]^{\frac{1}{m+n}} d\eta = C$$

$$2\pi\rho U_c^2 [\delta^n L^m]^{\frac{2}{m+n}} \int_0^\infty F^2 \eta d\eta = C$$

$$U_c^2 [\delta^n L^m]^{\frac{2}{m+n}} = C$$

$$U_c [\delta^n L^m]^{\frac{1}{m+n}} = C$$

Thus, we can deduce the following about the scaling of U_c:

$$U_c \sim [\delta^n L^m]^{-\frac{1}{m+n}}$$

Since for the no-swirl case, we know that the solution must collapse to $U_c\ \delta^{-1}$, we can assume that $n = 1$ and, for the case of $G_\theta = 0$, $m = 0$. This gives us the following relationship:

$$U_c \sim [\delta L^m]^{-\frac{1}{m+1}} \tag{11}$$

Logically, the exponent m should have some dependence on the swirl number, as the effects of swirl should be more pronounced in a flow with stronger swirl. While the swirling length scale L obviously has swirl dependence too, m must be a function of the swirl number to ensure that the swirling length scale drops out for the non-swirling case; we assume that $m(S) = 0$ for $S = 0$. We can find this relationship by rearranging the above expression:

$$U_c = C_1 [\delta L^m]^{-\frac{1}{m+1}}$$

$$\frac{1}{U_c^{m+1} L^m} = C_1 \delta$$

$$\frac{1}{(U_c L)^m} = C_1 U_c \delta$$

$$\frac{1}{C_1 U_c \delta} = (U_c L)^m$$

$$\log\left(\frac{1}{C_1 U_c \delta}\right) = m \log(U_c L)$$

$$m = C_2 \frac{\log\left(\frac{1}{U_c \delta}\right)}{\log(U_c L)} \tag{12}$$

Radial Velocity

An analagous analysis procedure can be applied to the scaling of the radial velocity. At the centerline, symmetry requires that the radial velocity vanish, that is $v = 0$ at $r = 0$. Thus, we will use the maximum radial velocity instead of the centerline radial velocity (as was done for the axial velocity analysis), assuming that the radial velocity at an arbitrary point is the product of the local maximum v_m and a similarity function $G(\eta)$.

$$v(r,x) = v_m(x) G(\eta)$$

Writing out the conservation of radial momentum flux using the similarity expressions for u and v results in the following:

$$\int_0^\infty \int_0^{2\pi} \rho uv r dr d\theta = C$$

$$2\pi\rho \int_0^\infty ruv dr = C$$

$$2\pi\rho \int_0^\infty u_c F v_m G(\eta) \eta \left[\delta L^m\right]^{\frac{1}{m+1}} \left[\delta L^m\right]^{\frac{1}{m+1}} d\eta = C$$

$$2\pi\rho u_c v_m [\delta^n L^m]^{\frac{2}{m+n}} \int_0^\infty FG\eta d\eta = C$$

$$u_c v_m [\delta^n L^m]^{\frac{2}{m+n}} = C$$

Assuming from above that n=1 and $U_c \sim [\delta L^m]^{-\frac{1}{m+1}}$, we obtain the scaling of v_m:

$$v_m \sim [\delta L^m]^{\frac{-1}{m+1}} \tag{13}$$

Azimuthal Velocity

The same procedure can be followed for azimuthal velocity. We assume that the azimuthal velocity can be expressed as the product of the maximum azimuthal velocity at a given point, $w(x)$, and a similarity function $H(\eta)$.

$$w(r,x) = w_m(x)H(\eta)$$

Introducing u, v and η into the momentum equation (10), we can simplify as follows:

$$\int_0^\infty \int_0^{2\pi} \rho r^2 uv d\theta dr = C$$

$$2\pi\rho \int_0^\infty r^2 uv dr = C$$

$$2\pi\rho \int_0^\infty \eta^2 [\delta L^m]^{\frac{2}{m+1}} U_c F W_m H [\delta L^m]^{\frac{1}{m+1}} = C$$

$$2\pi\rho U_c w_m [\delta^n L^m]^{\frac{3}{m+n}} \int_0^\infty FH\eta d\eta = 0$$

$$U_c w_m [\delta^n L^m]^{\frac{3}{m+n}} = C$$

Assuming from above that n=1 and $U_c \sim [\delta L^m]^{-\frac{1}{m+1}}$, we obtain the scaling of w_m:

$$w_m \sim [\delta L^m]^{\frac{-2}{m+1}} \tag{14}$$

Work by Shiri [4] and others suggests the same order relationship between the spreading rate of the asymptotic jet and the downstream distance; as in the non-swirling case, the jet grows linearly (albeit with a different rate constant). Chigier and Chervinsky suggested a linear relationship between swirl number and jet half-angle ($\delta = Ax$) although their data are not wholly consistent with this model, as seen in figure 2.

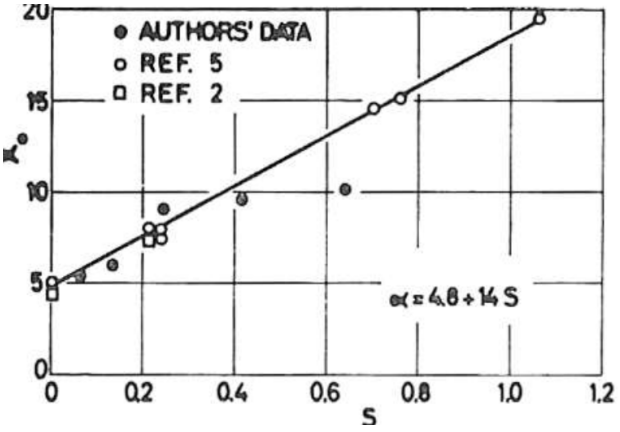

Fig. 2 : Half-angle of jets with varying degrees of swirl, from Chigier & Chervinsky [1]

Experimental data from several authors suggests that as in the case of the non-swirling jet, jet width δ increases linearly with downstream distance x [2][4][9]. Hence, in the above scaling analysis, δ can be replaced by x.
According to the solution, we can find that all velocity components decrease as the increase of x. And when x approaches to infinity, v decays as $1/x^{\frac{2}{m+1}}$, while u decays as $1/x^{\frac{1}{m+1}}$. Thus, the azimuthal velocity decays significantly before the axial velocity - specifically, the rate of decay of azimuthal velocity is the square of the rate of decay of axial velocity, as suggested by Ewing [9], meaning that it can be neglected at large downstream distances. At this point, the the flow should be almost indistinguishable from the non-swirling jet, except for a change in flow half-angle and virtual origin.

4 Comparison to Experimental Data

Although detailed experimental data on jets with varying swirl number are scarce in the literature, the work done by Chigier and Chervinsky provides an opportunity to evaluate the proposed scaling model. Their data cover a range of jets with swirl numbers from 0.066 to 0.640. Using equation 12 as derived above, it is possible to plot the swirling length scale exponent m against the swirl number S and deduce an approximate relationship. Doing this for the lower swirl numbers (up to 0.416, beyond which swirl enters the "crit-

ical" range), reveals a power-law relationship.

$$m = 2.29882\left(1 - \frac{1}{1+(\frac{x}{0.15741})^{1.01540}}\right) \quad (15)$$

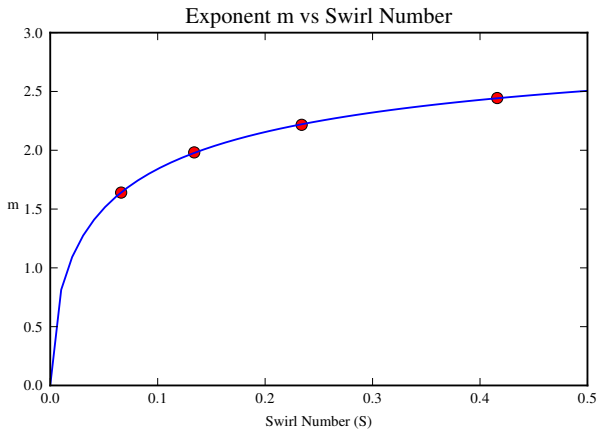

Fig. 3 : Power-law fit of scaling exponent m with respect to swirl number S.

.

In conjunction with equation 11, this function for m allows for comparison of the axial velocity decay profile for varying levels of swirl. This is shown below in figure 4.

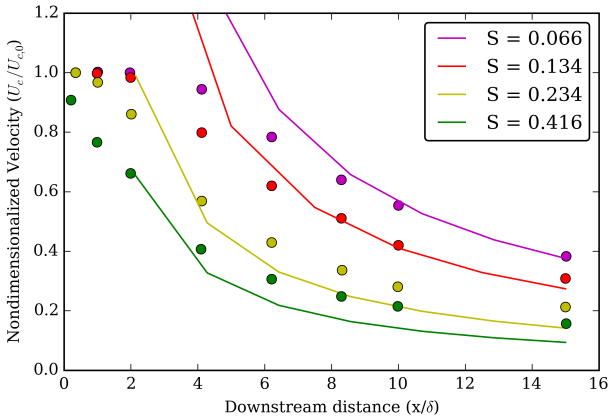

Fig. 4 : Comparison of scaling law with experimental data [1]

The overall trend of the predicted decay profile seems qualitatively accurate, although relatively minor discrepancies seem to manifest themselves at higher swirl numbers. The region in the immediate vicinity of the jet exit - perhaps 0-5 jet diameters - encompasses the development of the flow; that is, the flowfield is evolving to a point of self-similarity, but has yet to reach it (much like a more canonical similarity solution such as the Blasius boundary layer or the non-swirling jet). Farther downstream from this region, the flow seems to achieve self-similarity, and the predicted decay rates of axial velocity appear to provide an accurate model for the physical flow.

Note that a higher degree of accuracy may be possible with higher-fidelity experimental data. Accurately measuring the azimuthal jet velocity is challenging - as this velocity is an order of magnitude or more less than the axial velocity, it requires highly sensitive instrumentation with very precise positioning capabilities. Indeed, a contemporary paper by Pratte and Keffer [5] cited concerns with the accuracy of the Chigier and Chervinsky data and their swirl numbers. Although neither work calculates experimental uncertainty, it seems reasonable to suspect that the likely errors incurred by measuring azimuthal velocity profiles could have led to an inaccurate calculation of swirl number for one or more of the jets. Since the proposed similarity solution has a relatively strong dependence on the swirl number, a small discrepancy in this measurement could significantly change the expected scaling behaviour; in this case, more rigorous measurement of the azimuthal velocity may increase the accuracy of the similarity solution at higher swirl numbers.

In any case, it appears as though the proposed scaling of the axial velocity shows an accurate trend in the relatively far-field (where the flow would be expected to become self-similar). Without more experimental data to reference, it is difficult to put the proposed solution on a more solid footing, but the data from Chigier and Chervinsky suggest cause for optimism.

Using the value of m calculated from the axial decay data, it is also possible to apply the scaling model to the azimuthal velocity. Recalling equation (13) from above, we expect the following relation to hold:

$$w_m \sim [\delta L^m]^{\frac{-2}{m+1}} = x$$

Given the limited data available from Chigier and Chervinsky, we find a least-squares linear fit given by $w_m = -2.4x + 4.5$. This relationship is shown in the figure below.

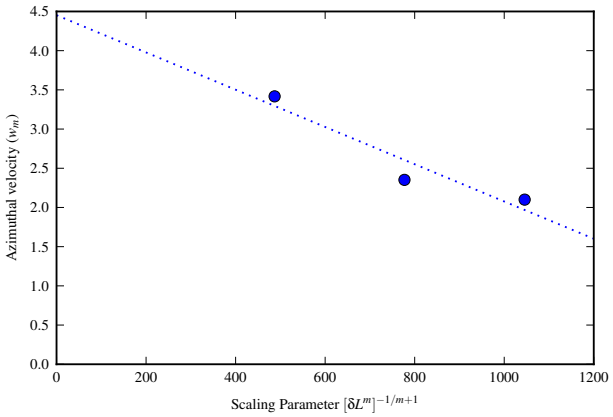

Fig. 5 : Azimuthal velocity measurements plotted against proposed scaling parameter [1]

.

Indeed, the scaling appears to be approximately linear (although with so few data points it is hard to draw firm conclusions). Unfortunately, the limited data from Chigier and Chervinsky are all that could be found in the literature. Regardless, it would appear that the azimuthal velocity decays an order of magnitude more rapidly than the axial or radial velocities.

5 Conclusions

Based on the available experimental data, the boundary layer scaling analysis presented in this work appears to offer a reasonable description of the far-field decay of swirling jets. As mentioned previously, the scarcity of detailed experimental data is a significant limitation, but the proposed solution based on a hybrid length scale comprised of the jet width δ and the swirling length scale L appears to match the available data with reasonable accuracy. The decay of axial velocity is well-predicted by the model for low and moderate values of the swirl number.

As Chigier and Chervinsky only provide three usable measurements for the decay of azimuthal velocity at sub-critical swirl numbers, it is difficult to draw a definite conclusion regarding the validity of this scaling theory. However, given the limitations of the available data (their scarcity as well as the equipment and instrumentation used to collect them), the fit between experimental data and the scaling solution is encouraging.

Overall, the scaling analysis presented in this report appears to present a credible model for the scaling of velocity profiles in a turbulent swirling jet. As other authors have noted, the scaling of mean axial and radial velocity profiles is linear in x as in the case of the non-swirling jet; the key differences for the flow of the swirling jet are a higher decay constant and the obvious addition of azimuthal velocity; this decays at a higher rate than the axial and radial velocities which is determined by the nondimensional swirl number.

The chief limitation of this theory is the lack of experimental data available for rigorous comparison. As noted above, several authors have studied the case of the swirling jet experimentally; however, the different methods used by each have resulted in a wide variety of relatively narrow data sets rather than the more comprehensive measurements of flow properties which are necessary to validate the proposed similarity solution. Few works in the literature study jets with a variety of swirl numbers; few present comprehensive data on the decay of each velocity component and profiles throughout the far field; only one work presents both in enough detail for practical use in this setting. In addition, different experiments in the literature use varying approaches to generate and measure swirl. All of these factors greatly complicate the evaluation of this theory, and further experimental work or a series of DNS computations could greatly elucidate the remaining uncertainty surrounding the question of the swirling jet. Nonetheless, based on the available data, the hybrid length scale similarity solution appears to be a relatively accurate model for describing the scaling of swirling turbulent jets in the mid- to far-field domain.

6 Acknowledgements

The author would like to thank Professor Greg Blaisdell for his guidance during the course of this work, Professor Jonathan Poggie for being a supportive advisor and mentor, and fellow student Ang Li for his unpublished contributions to the project. The author would also like to express his gratitude to the American Institute of Aeronautics and Astronautics (AIAA) for choosing this paper for submission to ICAS 2018.

7 References

References

[1] Chigier N and Chervinsky A. "Experimental Investigation of Swirling Vortex Motion in Jets," *Journal of Applied Mechanics*, Vol. 34, No. 2, pp.443-451, 1967.

[2] Facciolo L, Tillmark N, Talamelli, A. and Henrik, A.P."A Study of Swirling Turbulent Pipe and Jet Flows," *Physics of Fluids*, Vol.19, No.3, pp.35-105, 2007

[3] Rose, W. "A Swirling Round Turbulent Jet: 1 - Mean-Flow Measurements," *Journal of Applied Mechanics* 29.4 pp. 615-625, 1962.

[4] Shiri A, George W, and Naughton W. "An Experimental Study of the Far-Field of Incompressible Swirling Jets," *AIAA Journal*, Vol. 46, No, 8. pp. 2002-2009, 2006.

[5] Pratte B and Keffer J. "The Swirling Turbulent Jet," *Journal of Basic Engineering*, 94.4, pp. 739-747, 1972. ASME Paper 72-FE-18.

[6] Ruith M, Chen P, Meiburg E, and Maxworthy T. "Three-dimensional vortex breakdown in swirling jets and wakes: direct numerical simulation," *Journal of Fluid Mechanics* Vol. 486, pp. 331-378, 2003.

[7] Billant P, Chomaz J, and Heurre P. "Experimental Study of Vortex Breakdown in Swirling Jets," *Journal of Fluid Mechanics*, Vol. 376 pp. 183-219, 1998.

[8] Escudier M and Keller J. "Vortex Breakdown: a Two-Stage Transition," Brown Boveri Research Center, Baden, Switzerland, 1983.

[9] Ewing D."Decay of Round Turbulent Jets with Swirl," *Fourth International Symposium on Engineering Turbulence Modelling and Experiments*, pp. 461-470, Ajaccio, Corsica, 1999.

[10] Batchelor G. "Steady Axisymmetric Flow with Swirl," *An Introduction to Fluid Dynamics*, Cambridge University Press, Cambridge, 2002.

8 Contact Author Email Address

geoffreymgandrews@gmail.com

Copyright Statement